

Theoretical investigation of the $\text{H} + \text{HD} \rightarrow \text{D} + \text{H}_2$ chemical reaction for astrophysical applications: A state-to-state quasi-classical study

Cite as: J. Chem. Phys. **153**, 081102 (2020); <https://doi.org/10.1063/5.0017697>

Submitted: 10 June 2020 . Accepted: 08 July 2020 . Published Online: 25 August 2020

Duncan Bossion , Steve Ndengué , Hans-Dieter Meyer , Fabien Gatti, and Yohann Scribano 



View Online



Export Citation



CrossMark

Lock-in Amplifiers
up to 600 MHz



Theoretical investigation of the $\text{H} + \text{HD} \rightarrow \text{D} + \text{H}_2$ chemical reaction for astrophysical applications: A state-to-state quasi-classical study

Cite as: J. Chem. Phys. 153, 081102 (2020); doi: 10.1063/5.0017697

Submitted: 10 June 2020 • Accepted: 8 July 2020 •

Published Online: 25 August 2020



View Online



Export Citation



CrossMark

Duncan Bossion,^{1,a)} Steve Ndengué,² Hans-Dieter Meyer,³ Fabien Gatti,⁴ and Yohann Scribano^{1,b)}

AFFILIATIONS

¹Laboratoire Univers et Particules de Montpellier, Université de Montpellier, UMR-CNRS 5299, 34095 Montpellier, France

²ICTP-East African Institute for Fundamental Research, University of Rwanda, Kigali, Rwanda

³Physikalisch-Chemisches Institut, Universität Heidelberg, Im Neuenheimer Feld 229, D-69120 Heidelberg, Germany

⁴Institut de Sciences Moleculaires d'Orsay, UMR-CNRS 8214, Université Paris-Saclay, 91405 Orsay, France

^{a)}Now at: Department of Chemistry, University of Rochester, 120 Trustee Road, Rochester, New York 14627, USA.

^{b)}Author to whom correspondence should be addressed: yohann.scribano@umontpellier.fr

ABSTRACT

We report a large set of state-to-state rate constants for the $\text{H} + \text{HD}$ reactive collision, using Quasi-Classical Trajectory (QCT) simulations on the accurate H_3 global potential energy surface of Mielke *et al.* [J. Chem. Phys. **116**, 4142 (2002)]. High relative collision energies (up to $\approx 56\,000$ K) and high rovibrational levels of HD (up to $\approx 50\,000$ K), relevant to various non thermal equilibrium astrophysical media, are considered. We have validated the accuracy of our QCT calculations with a new efficient adaptation of the Multi Configuration Time Dependent Hartree (MCTDH) method to compute the reaction probability of a specific reactive channel. Our study has revealed that the high temperature regime favors the production of H_2 in its highly rovibrationally excited states, which can de-excite radiatively (cooling the gas) or collisionally (heating the gas). Those new state-to-state QCT reaction rate constants represent a significant improvement in our understanding of the possible mechanisms leading to the destruction of HD by its collision with a H atom.

Published under license by AIP Publishing. <https://doi.org/10.1063/5.0017697>

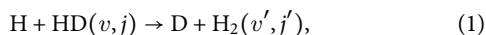
I. INTRODUCTION

H_2 and its main isotopologue HD are the main cooling species of the low-metallicity clouds and, thus, are key elements in the formation process of the first baryonic objects in the Universe such as Pop-III stars (see, for example, the review of Bromm and Larson¹). Although H_2 is the most abundant diatomic molecule, it can be a less efficient cooling species than its deuterated analogue HD (which can cool down the primordial gas² below 100 K) because the rotational energy interval is larger for H_2 than for HD. Moreover, the non-zero permanent electric dipole moment of HD increases the cooling efficiency of this isotopologue over H_2 . This was confirmed by the first quantum calculation performed by Flower *et al.*³ Thus, HD may well play an important role in the cooling process of the early Universe although we should bear in mind the low cosmological fractional abundance⁴ of HD relative to H_2 ($\text{D}/\text{H} \approx 10^{-5}$). For low

density astrophysical media ($n_{\text{H}} < 10^3 \text{ cm}^{-3}$), the relative population of the HD levels is far from following a Boltzmann distribution. In this case, a correct evaluation of the cooling function requires the correct values of the rovibrational level population. This latter requires the inclusion of the rovibrational structure in the chemical kinetic network, which itself requires the knowledge of accurate micro-physics data of all possible transitions among levels due to radiative and collisional processes. Thus, accurate collisional rate constants for inelastic and reactive processes are needed in order to correctly determine the HD cooling function.

The non-reactive collision (inelastic process) between HD and the H collider has been studied by Flower and Roueff⁵ or Wrathmall *et al.*⁶ using a non-reactive quantum method in order to derive inelastic rotational excitation rate constants. More recently, this study was revisited by Desrousseaux *et al.*⁷ using the quantum reactive scattering approach including the reactive channel up to 1000 K.

In this study, the authors have shown that the inclusion of the reactive channel in quantum inelastic formalism is necessary, even for low temperatures, in order to provide accurate state-to-state inelastic reaction rates. They also showed that at relatively low translational temperature ($T < 1000$ K), the inelastic process dominates the reactive channel but in the same time, they concluded that reactive scattering calculations are required for higher temperature (roughly until 5000 K) considering explicitly the reactive channel. Indeed, in this temperature regime of few thousands kelvins, the population of the excited rovibrational level becomes significant, and thus, a complete knowledge at the state-to-state level of the reactive process:



is necessary in modeling the HD cooling function.⁸ However, the cost of quantum close-coupling reactive scattering calculations is numerically intractable due to the very large number of channels, which should be considered in such situation. Only a limited number of quantum simulations have been performed in the past^{9,10} for this specific chemical reaction. Those previous studies were focused mainly on the initial rovibrational ground state of HD or in some low-excited rovibrational levels, and they did not provide a full reaction rates analysis. This has motivated us to use a more approximated but numerically tractable approach, the Quasi-Classical Trajectory (QCT) method, to produce a large number of useful rate constants for astrophysical applications. We have indeed used this approach in a recent work to study the reverse reaction $\text{D} + \text{H}_2$, and we have shown that such QCT method was reliable for astrophysical applications in regimes where quantum effects are not too relevant (as, for example, high temperature regime or low temperature regime considering a high initial rovibrational state of the reactant). Within this work, we have neglected the Geometric Phase (GP) effect even if we are looking for high collisional energy. Indeed, as mentioned by Kendrick *et al.*,¹¹ previous works^{12,13} on $\text{H} + \text{H}_2$ (and its isotopic variants) collisions, at high total energy (greater than ~ 2 eV) and for a large value of total angular momentum J , have highlighted rapid oscillations in differential cross section as a function of scattering angle due to the GP effect. However, these rapid oscillations average out and vanish in the integral cross sections¹⁴ and, thus, should not be too much relevant for the calculation of reaction rate constants.

The paper is organized as follows: Section II provides a brief description of the employed methodology for our scattering calculations. In Sec. III, we present the results. Concluding remarks are drawn in Sec. IV.

II. REACTIVE SCATTERING CALCULATIONS

A. QCT method

The Quasi classical Trajectory (QCT) calculations were performed solving classical Hamiltonian equations. We have solved those equations using standard approaches as developed by Truhlar and Muckerman,¹⁵ more details can be found in previous papers^{16,17} of some of us, and we just give below a brief summary. Propagation of trajectories was performed using an adaptive time-step size Runge–Kutta solver.¹⁸ The initial and final rovibrational internal energies, respectively, $\epsilon_{v,j}$ and $\epsilon_{v',j'}$ of the HD and H_2 fragments are computed using the Fourier Grid Hamiltonian (FGH) method of Marston and Balint-Kurti.¹⁹ We performed calculations

for fixed collisional energies E_c , all the other collision parameters being sampled using the Monte Carlo algorithm according to their own probability distribution.¹⁶

For a diatomic product, a final pseudo-quantum (continuous) rotational number \tilde{j} is taken using the total angular momentum of the diatomic, and the vibrational pseudo-quantum number \tilde{v} is determined using the Wentzel–Kramer–Brillouin quantization condition.¹⁵ We use the histogram binning method,¹⁵ and hence, the rovibrational quantum number (v', j') is defined as the nearest integer of the pseudo-quantum rovibrational number (\tilde{v}, \tilde{j}) . A bin is specified for each rovibrational final quantum number. Quasi-bound and dissociated trajectories are stored in a specific bin.

The state-to-state cross section is defined from a given initial $\text{HD}(v, j)$ state to a final $\text{H}_2(v', j')$ state as

$$\sigma_{v',j' \leftarrow v,j}(E_c) = \pi \left[b_{\max}^{v,j}(E_c) \right]^2 \frac{N_{\text{reac}}^{v',j'}(E_c)}{N_{\text{tot}}^{v,j}(E_c)}, \quad (2)$$

where E_c is the initial relative collision energy, $N_{\text{tot}}^{v,j}(E_c)$ is the total number of trajectories started in the rovibrational state $\text{HD}(v, j)$, and $N_{\text{reac}}^{v',j'}(E_c)$ is the trajectory count in the histogram bin labeled (v', j') for the product of interest, here H_2 . In the above equation, b_{\max} is the maximum value of the impact parameter, which is sufficiently large that no reaction takes place beyond it.

The state-to-state rate constant is determined assuming a Maxwellian distribution of the collision energy at temperature T ,

$$k_{v',j' \leftarrow v,j}(T) = \left(\frac{8}{\pi \mu k_B^3 T^3} \right)^{1/2} \int_0^\infty \sigma_{v',j' \leftarrow v,j}(E_c) E_c e^{-\frac{E_c}{k_B T}} dE_c, \quad (3)$$

with the Boltzmann constant being k_B and μ being the reduced mass of the H–HD system.

A state-specific rate constant for the initial state (v, j) of HD is obtained through a summation over all energetically accessible product states (for the channel of interest), namely,

$$k_{vj}(T) = \sum_{v',j'} k_{v',j' \leftarrow v,j}(T). \quad (4)$$

B. Computational details

Within this work, all calculations use the accurate H_3 global potential energy surface of Mielke *et al.*,²⁰ as in our previous study of the $\text{D} + \text{H}_2$ and $\text{H} + \text{H}_2$ reactions.^{16,17} The impact parameter has a b^2 distribution in the $[0, b_{\max}^{v,j}]$ range in order to have the best behavior of the maximal impact parameter, and small batches of 200 trajectories are launched prior to the propagation in order to get points of the $b_{\max}^{v,j}(E_c)$ function. Once this specific maximal impact parameter is computed on a grid of collisional energy, an interpolation was done to get its value for any further required value of E_c . The reactants have an initial relative distance of $30 a_0$, and the trajectories are propagated until any two of the three internuclear distances are above $31 a_0$. During the propagation of classical trajectories, the relative precision over the total energy and total angular momentum is monitored to be better than 10^{-7} .

Batches of 70 000–100 000 trajectories were propagated for 53 distinct relative collision energies E_c between 10 K and 60 000 K

for each initial rovibrational state (v, j) of HD. A total of 339 initial rovibrational states have been examined, spanning HD internal energies up to $\approx 50\,000$ K, with the highest rovibrational levels (v, j) being (0,35), (1,33), (2,32), (3,30), (4,28), (5,27), (6,25), (7,23), (8,21), (9,19), (10,17), (11,14), (12,11), (13,8), and (14,1). This represents, with the 301 final rovibrational states of H_2 , (0,31), (1,30), (2,28), (3,27), (4,25), (5,23), (6,22), (7,20), (8,18), (9,16), (10,14), (11,12), (12,10), (13,7), (14,3), a total of 102 039 computed state-to-state rate constant values for each translational temperature. A comprehensive list of the computed results is provided in the [supplementary material](#).

III. RESULTS AND DISCUSSIONS

A. Benchmarking QCT simulations with MCTDH calculations

Since a time-independent quantum close-coupling calculation is not tractable for the high temperature of interest, we assess the accuracy of our QCT calculations by comparing it with results from Multi Configuration Time Dependent Hartree (MCTDH) calculations^{21,22} (as implemented in the Heidelberg MCTDH package²³). Using this efficient wave-packet method, we are able to establish a set of reference values for the reaction $\text{H} + \text{HD}(v = 0, j = 0) \rightarrow \text{D} + \text{H}_2$ over a limited collision energy range, i.e., below 23 200 K.

We recall below the definition of the state-specific quantum cross section,

$$\sigma_{vj}(E_c) = \sum_{m=-j}^j \sum_{|m|}^{J_{\max}} \frac{\pi}{\kappa_{vj}^2} \frac{2J+1}{2j+1} P_{v|j|m}^J(E_c), \quad (5)$$

for the initial (v, j) states, where m is the quantum number relative to the projection of the rotational angular momentum of the target diatom on its axis and κ_{vj} is the wavevector relative to the initial diatom eigenstate (v, j) [see Eq. (18) of Ref. 24 for its definition]. The reaction probability $P_{v|j|m}^J(E_c)$ is extracted from the final MCTDH wavepacket, following the general procedure of Sukiasyan and Meyer.²⁴ We thus have here a Jacobi coordinate system with r being the H–D interatomic distance of the diatomic reactant, R being the distance from the center of mass of HD and the H atom, and θ being the angle between the directions of r and R . As it was done in that work, we used two Complex Absorbing Potentials (CAPs) to absorb both the reactive and non-reactive parts of the flux. The intensity of the CAPs was obtained from the program *plcap* implemented in the Heidelberg MCTDH package,²³ and the position of the CAP was selected as in similar MCTDH studies on $\text{H} + \text{H}_2$ isotopologues so as to ensure the convergence of the calculations. The length, intensity, and order of the CAPs along R and r are $4.0/8.0 \times 10^{-4}/3$ and $4.0/4.7 \times 10^{-4}/3$, respectively. The parameters used for our calculations are reported in Table I. For the calculations presented here, the initial wavepacket is located at 6 bohrs with a width of 0.25 and a momentum of -8 a.u. The energy distribution thus covers the 0.01 eV–2.0 eV range. Here, as HD is a heteronuclear diatom, the reactive process may lead to either the $\text{H}_2 + \text{D}$ or the $\text{HD} + \text{H}$ products, depending on how the breakup and the subsequent re-arrangement is done. The flux going to one channel or the other can then be controlled by the parameter θ as for $\theta > \pi/2$, the $\text{HD} + \text{H}$ channel will take place and for $\theta < \pi/2$, the competing channel $\text{H}_2 + \text{D}$ will be populated. Using a step-operator

TABLE I. Parameters of the primitive basis used for the MCTDH scattering calculations. FFT stands for the fast Fourier transform. KLeg is the K-Legendre DVR.²⁴ The units for distance and angle are bohrs and radians, respectively.

| Coordinate | Primitive basis | Number of points | Range | Size of SPF basis |
|------------|-----------------|------------------|-----------|-------------------|
| R | FFT | 68 | 1.0–10.0 | 20 |
| r | FFT | 48 | 0.6–8.0 | 18 |
| θ | KLeg | 48 | 0– π | 24 |
| k | K | 21 | –10 to 10 | |

within the MCTDH flux analysis, we are then able to separate the two contributions and obtain for each value of J the probability. To our knowledge, this is the first time this technique is used within the MCTDH approach: in a forthcoming publication, a more extensive description will be presented. The state-specific quantum rate constant is obtained as the integral of Eq. (5) over the collision energy E_c ; the resulting expression, similar to Eq. (3), is thus integrated numerically.

The MCTDH calculations are performed with about 8640 configurations. To ensure convergence of the cross section [Eq. (5)], the maximum value of the total angular momentum is $J_{\max} = 40$ for all collisional energies, that is, up to 23 200 K. In Fig. 1, we report the state-specific rate constants for the reaction of H with $\text{HD}(v = 0, j = 0)$. Both the quantum and classical rate constants increase rapidly with the translational temperature as expected for an abstraction reaction with a significant energy barrier (here, the barrier height is estimated²⁰ to be near to ~ 3500 cm^{-1}). The classical rate constant, obtained with 70 000 trajectories per collision energy, appears to be quite close to the exact quantum rate constant over the whole temperature range displayed here. Looking at higher temperatures,

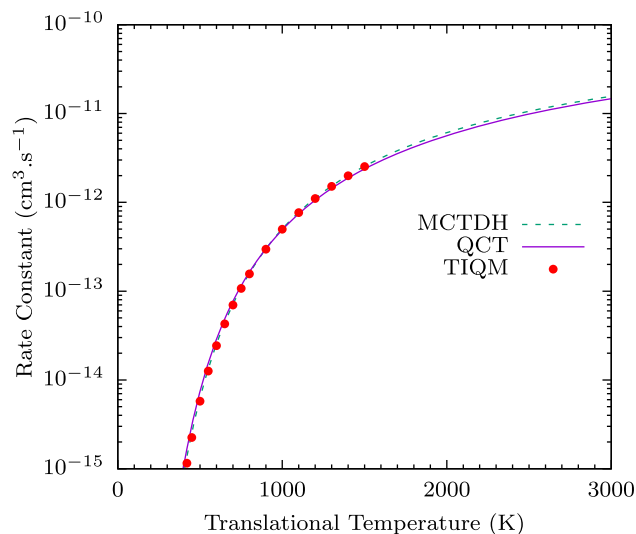


FIG. 1. Rate constant for the reaction $\text{H} + \text{HD}(v = 0, j = 0) \rightarrow \text{D} + \text{H}_2$ as a function of the translational temperature: a comparison of the QCT result (solid line) with the MCTDH quantum reference calculation (dashed line) and TIQM calculations (red dots) of Desrousseaux *et al.*⁷

the two curves remain close to each other, but some slight difference appears likely due to the fact that cross sections computed with MCTDH at higher energy (above 1.9 eV) are not as accurate as the lower energy cross sections because of the low amplitude of the energy distribution, which affects the collision probabilities. Otherwise, the Time Independent Quantum Mechanical (TIQM) calculations of Desrousseaux *et al.*,⁷ also reported in Fig. 1, are in very good agreement with our MCTDH and QCT results. This agreement between the TIQM and QCT simulations is always satisfactory when we consider an initial rotational excited state ($v = 0, j = 8$), as reported in Fig. 2. Thus, the agreement between the QCT and quantum rate constants for the reaction of H with HD at those temperatures is already quite satisfactory and can only improve at higher temperatures and for higher initial rovibrational states of the HD target.

B. Rovibrational state-to-state reactive rate constants

In Fig. 3 are reported QCT rate constants for the reaction $\text{H} + \text{HD}(v = 0, j = 0) \rightarrow \text{H}_2(v', j') + \text{D}$. We can globally observe that increasing temperature tends to favor high rotational states, while the vibrational excitation is much less favored. As an illustration, we can see in Fig. 3 that for the highest temperature considered, the most populated states are $\text{H}_2(v = 0, j = 3)$ and $\text{H}_2(v = 0, j = 8)$ with a relatively high rate constant, reaching a plateau at $\approx 4 \times 10^{-12} \text{ cm}^3 \text{ s}^{-1}$. For the same temperature, the rate constant of the vibrational excited state $\text{H}_2(v = 1, j = 0)$ is lower by more than an order of magnitude.

We report in Fig. 4 the state-to-state rate constants for the reactive collision of H with HD in an excited rotational state of its ground vibrational state. The main reactive transitions for translational temperatures of a few thousand kelvins lead to the formation of H_2 molecules with internal energy lower than the initial HD internal energy. We observed this behavior, for example, in the transition

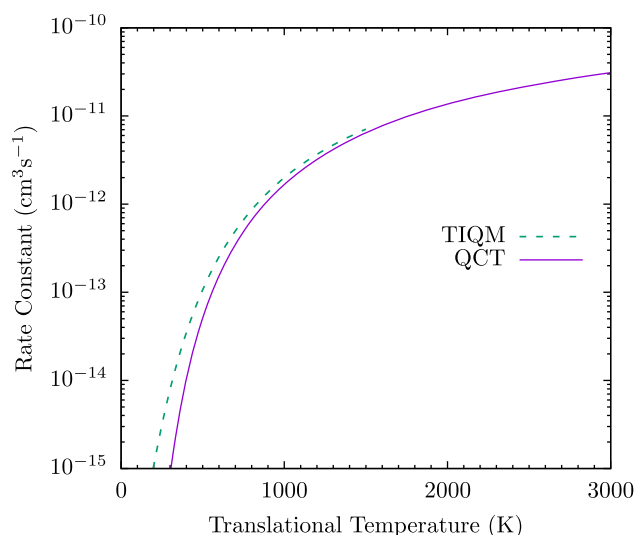


FIG. 2. Rate constant for the reaction $\text{H} + \text{HD}(v = 0, j = 8) \rightarrow \text{D} + \text{H}_2$ as a function of the translational temperature: a comparison of the QCT result (solid line) with the TIQM calculations (dashed line) of Desrousseaux *et al.*⁷

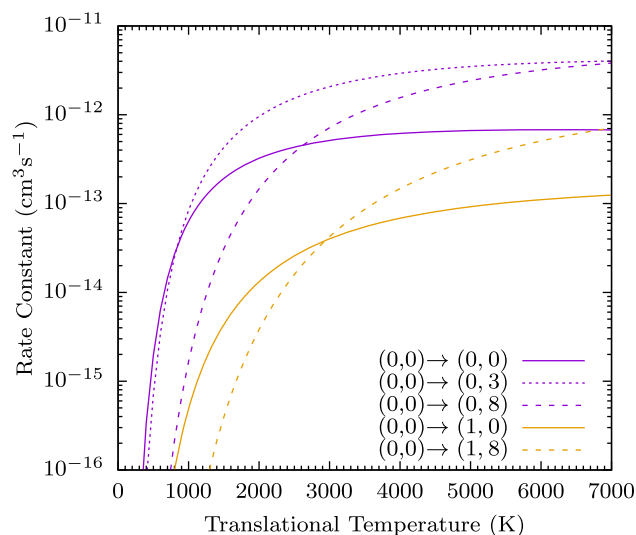


FIG. 3. State-to-state rate constants for the reactive collision $\text{H} + \text{HD}(v = 0, j = 0) \rightarrow \text{H}_2(v', j') + \text{D}$.

starting from $\text{HD}(v = 0, j = 9)$ and leading to $\text{H}_2(v' = 0, j' = 4)$ for which $\epsilon_{v'j'} - \epsilon_{vj} = 4876 \text{ cm}^{-1}$ (or 7015 K). Increasing the translational temperature leads to H_2 molecules with internal energy closer to the initial HD internal energy as $\text{H}_2(v' = 0, j' = 10)$ is also efficiently formed with a relatively high rate constant, reaching a plateau at $\approx 6 \times 10^{-12} \text{ cm}^3 \text{ s}^{-1}$. We also observe that reactions with large exoergicity are not necessarily dominant. This is, for example, observed in the reaction from $\text{HD}(v = 0, j = 9)$ leading to the formation of $\text{H}_2(v' = 0, j' = 0)$ for which $\epsilon_{v'j'} - \epsilon_{vj} = 3536 \text{ cm}^{-1}$ (5088 K). Hence, dominant reactive transitions are only slightly exoergic, a usual characteristic that can be explained with simple energy gap law.²⁵ From

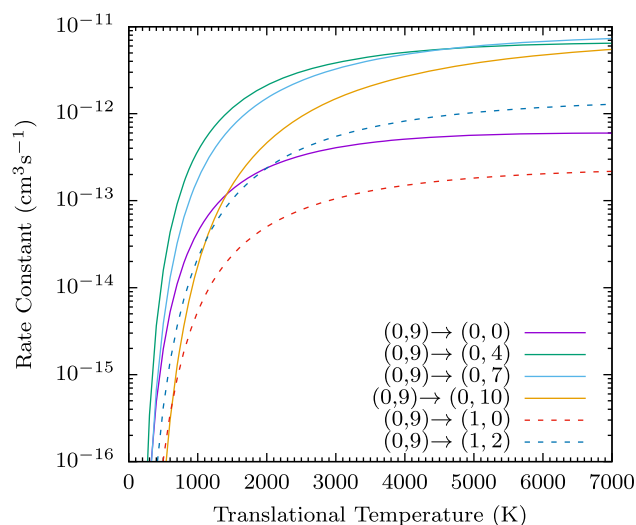


FIG. 4. State-to-state rate constants for the reactive collision of the H atom with HD in its ground vibrational state. From $\text{H} + \text{HD}(v = 0, j) \rightarrow \text{H}_2(v', j') + \text{D}$.

the ground vibrational state even at high translational temperature, endoergic reactions [here, $\text{H}_2(v' = 0, j' = 10)$] are not dominant, but from 5000 K, they get the same magnitude than the exoergic reactive transitions.

Increasing the translational temperature will not lead to a higher vibrational excited level. Indeed, we can see that from ≈ 5000 K, the transition leading to $\text{H}_2(v' = 1, j' = 2)$ is an order of magnitude more efficient than to the ground rotational state ($v' = 1, j' = 0$). We observe a similar effect for the rate constant leading to $\text{H}_2(v' = 0, j' = 7)$, which crosses the one leading to $\text{H}_2(v' = 0, j' = 4)$ around 4500 K. We can conclude that, as already observed in our previous study for the reverse reaction,¹⁷ the product (here, H_2) is preferably formed with high rotational excitation, while vibrational excitation is less likely.

In Fig. 5, we report the behavior of reaction rates for the highly excited rovibrational initial state of HD. As noticed previously, low final H_2 rotational states are less efficiently formed at moderate-to-high temperatures, and excited H_2 states are efficiently formed for rovibrational reactive transitions as the reactions lead to $\text{H}_2(v' = 2, j' = 11)$ and $\text{H}_2(v' = 3, j' = 11)$. At low temperature, we note that the main reactive transitions are purely rotational; hence, a reactive transition is not more efficient with its exoergicity (which would lead otherwise to transitions toward lower rovibrational H_2 states).

One important remark is that since rovibrationally excited HD molecules lead efficiently to a rovibrationally excited H_2 product, we can consider that this reactive process will enhance the cooling efficiency of the molecular cloud (through rovibrational radiative and collisional transitions of the newly formed H_2 molecule).

In complement to what we have discussed above on some individual representative state-to-state rate constants, in Fig. 6, we show a scatter plot of a large number of state-to-state rate constant values (5101 randomly selected values of the 102 039 actually computed) for three translational temperatures, i.e., $T = 500$ K, 5000 K, and 10 000 K. The three ensembles of points, distributed over the energy difference between the product and reactant rovibrational states, are

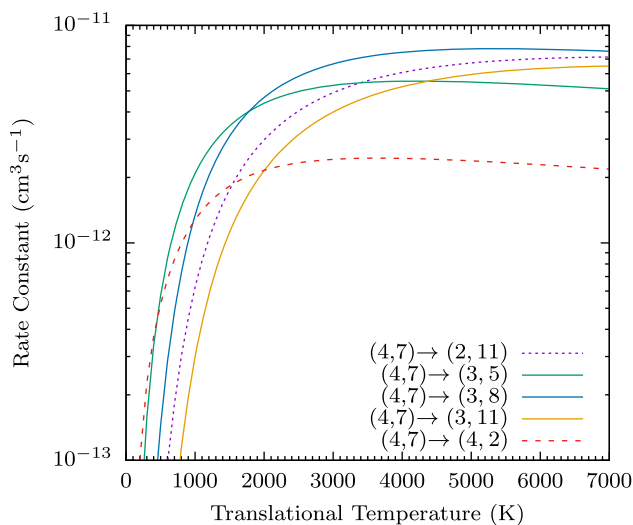


FIG. 5. State-to-state rate constants for the reactive collision of the H atom with HD in a highly excited rovibrational state. From $\text{H} + \text{HD}(v, j) \rightarrow \text{H}_2(v', j') + \text{D}$.

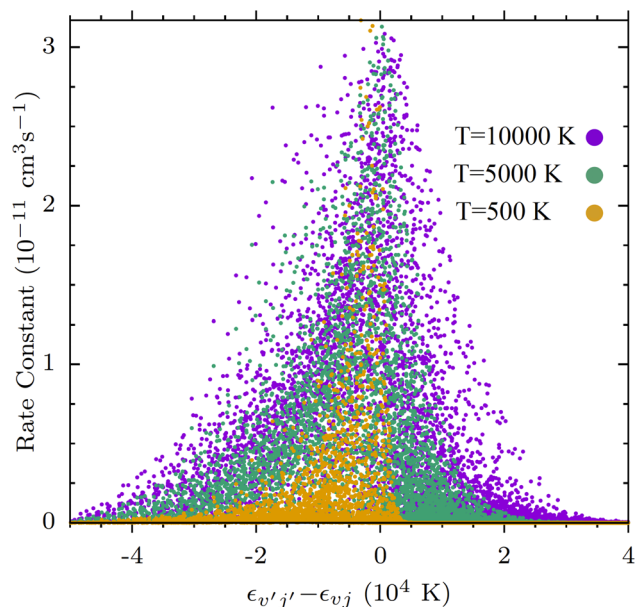


FIG. 6. QCT rate constant scatter plot for the reaction $\text{H} + \text{HD}(v, j) \rightarrow \text{H}_2(v', j') + \text{D}$ for three translational temperatures. The horizontal axis represents the energy difference between the product and reactant rovibrational levels. The rate constants for 5000 K and 10 000 K have been multiplied by 2.0 and 2.6, respectively. For clarity, only 5101 (randomly selected) points of the 102 039 actually computed are shown.

centered at energy resonance and expand over large (negative and positive) energy differences. We can observe that the larger the temperature, the wider the expansion—except for the distribution at 500 K, which shows a sharp falloff around +4000 K.

We thus observe that if larger collision energies are available to the system, higher temperatures allow for more off-resonance reactions (distributed symmetrically around the resonance), while the reverse is true for lower temperatures, as seen in Fig. 6. Moreover, at sufficiently low temperatures, a cross section energy threshold may come into play, translating into an abrupt slope in the reaction rate, as exemplified in Fig. 6 for $T = 500$ K. For most of the state-to-state reactive transitions, the vibration is more efficient than the rotation in promoting the reaction. We also observed that products are formed in rotationally excited states, usually higher than the initial reactant's rotational level, but at a lower vibrational level. It is to be noted, however, that for such reactive collisions, $\Delta v = v' - v$ is usually fairly small.

To summarize, in the reaction $\text{H} + \text{HD} \rightarrow \text{H}_2 + \text{D}$, quasi-resonant rovibrational state-to-state rates are favored at low translational temperatures, while off-resonance reactions become more important as temperature is raised.

IV. CONCLUSION

We have presented a large set of state-to-state QCT rate constants for the $\text{H} + \text{HD}$ reactive collision. Our calculations explore high collisional and internal energies, currently inaccessible to fully close-coupling quantum reaction dynamics calculations. A total of 339 rovibrational states of the HD target have been examined,

resulting in 102 039 computed state-to-state rate constants for each translational temperature. This very large number of computed rate constants allows us to derive general conclusions about the reaction mechanism. Quasi-resonant rovibrational state-to-state H_2 products are favored at low translational temperatures, while off-resonance reactions become more important at higher temperatures. The H_2 product is preferably formed with high rotational excitation, while vibrational excitation is much less likely. Since this chemical reaction tends to form molecular hydrogen in rovibrational excited states, it participates indirectly (but efficiently) to increase the cooling in molecular gas.

Those new results are relevant for any further chemical kinetic network involving collisional processes of HD with H at the state-to-state level and explicitly considering the rovibrational structure of the reactants/products. Furthermore, those new results should also be useful for astrophysical media such as for photon dominated regions (PDRs) illuminated by a strong radiation field,²⁶ which can promote molecules to high rovibrational energy levels.

SUPPLEMENTARY MATERIAL

See the [supplementary material](#) for a comprehensive list of the computed rovibrational state-to-state rate constants for the reaction $\text{H} + \text{HD}(v, j) \rightarrow \text{D} + \text{H}_2(v', j')$.

ACKNOWLEDGMENTS

This work was supported by the “Programme National Physique et Chimie du Milieu Interstellaire” (PCMI) of CNRS/INSU with INC/INP co-funded by CEA and CNES. Y.S. and D.B. would like to thank for support from the High Performance Computing Platform MESO@LR at the University of Montpellier and from the Computing Center of the “Institut National de Physique Nucléaire” (IN2P3). Y.S. would like to thank F. Lique for fruitful discussions and for sharing TIQM data.

DATA AVAILABILITY

The data that support the findings of this study are available within the [supplementary material](#), which contains a comprehensive list of the computed rovibrational state-to-state rate constants for the reaction $\text{H} + \text{HD}(v, j) \rightarrow \text{H}_2(v', j') + \text{D}$.

REFERENCES

- ¹V. Bromm and R. B. Larson, *Annu. Rev. Astron. Astrophys.* **42**, 79 (2004).
- ²D. Galli and F. Palla, *Annu. Rev. Astron. Astrophys.* **51**, 163 (2013).
- ³D. R. Flower, J. Le Bourlot, G. Pineau des Forêts, and E. Roueff, *Mon. Not. R. Astron. Soc.* **314**, 753 (2000).
- ⁴D. Puy and M. Signore, *New. Astron.* **3**, 247 (1998).
- ⁵D. R. Flower and E. Roueff, *Mon. Not. R. Astron. Soc.* **309**, 833 (1999).
- ⁶S. A. Wrathmall, A. Gusdorf, and D. R. Flower, *Mon. Not. R. Astron. Soc.* **382**, 133 (2007).
- ⁷B. Desrousseaux, C. M. Coppola, M. V. Kazandjian, and F. Lique, *J. Phys. Chem. A* **122**, 8390 (2018).
- ⁸A. Lipovka, R. Núñez-López, and V. Avila-Reese, *Mon. Not. R. Astron. Soc.* **361**, 850 (2005).
- ⁹S. A. Harich, D. Dai, X. Yang, S. D. Chao, and R. T. Skodje, *J. Chem. Phys.* **116**, 4769 (2002).
- ¹⁰S. D. Chao, S. A. Harich, D. X. Dai, C. C. Wang, X. Yang, and R. T. Skodje, *J. Chem. Phys.* **117**, 8341 (2002).
- ¹¹B. K. Kendrick, J. Hazra, and N. Balakrishnan, *Nat. Commun.* **6**, 7918 (2015).
- ¹²J. C. Juanes-Marcos, S. C. Althorpe, and E. Wrede, *Science* **309**, 1227 (2005).
- ¹³F. Bouakline, S. C. Althorpe, and D. Peláez Ruiz, *J. Chem. Phys.* **128**, 124322 (2008).
- ¹⁴J. C. Juanes-Marcos and S. C. Althorpe, *J. Chem. Phys.* **122**, 204324 (2005).
- ¹⁵D. G. Truhlar and J. T. Muckerman, *Atom-Molecule Collision Theory: A Guide for the Experimentalist* (R. B. Bernstein, 1979).
- ¹⁶D. Bossion, Y. Scribano, F. Lique, and G. Parlant, *Mon. Not. R. Astron. Soc.* **480**, 3718 (2018).
- ¹⁷D. Bossion, Y. Scribano, and G. Parlant, *J. Chem. Phys.* **150**, 084301 (2019).
- ¹⁸W. H. Press, S. A. Teukolsky, W. T. Vetterling, and B. P. Flannery, *Numerical Recipes in C: The Art of Scientific Computing* (Cambridge University Press, 1986).
- ¹⁹C. C. Marston and G. G. Balint-Kurti, *J. Chem. Phys.* **91**, 3571 (1989).
- ²⁰S. L. Mielke, B. C. Garrett, and K. A. Peterson, *J. Chem. Phys.* **116**, 4142 (2002).
- ²¹H.-D. Meyer, U. Manthe, and L. S. Cederbaum, *Chem. Phys. Lett.* **165**, 73 (1990).
- ²²*Multidimensional Quantum Dynamics: MCTDH Theory and Applications*, edited by H. D. Meyer, F. Gatti, and G. A. Worth (Wiley VCH, Weinheim, 2009).
- ²³G. A. Worth, M. H. Beck, A. Jäckle, and H.-D. Meyer, The MCTDH Package, Version 8.2, 2000; H.-D. Meyer, Version 8.3, 2002, Version 8.4, 2007, current version: 8.4.18, 2019; See <http://mctdh.uni-hd.de/> for a description of the MCTDH package.
- ²⁴S. Sukyasian and H.-D. Meyer, *J. Phys. Chem. A* **105**, 2604 (2001).
- ²⁵R. D. Levine, *Annu. Rev. Phys. Chem.* **29**, 59 (1978).
- ²⁶F. Le Petit, E. Roueff, and J. Le Bourlot, *Astron. Astrophys.* **390**, 369 (2002).